*18th International Symposium Ballistic*s, San Antonio, TX, Nov. 1999.

Hypervelocity Jet Penetration of Porous Materials

Authors: William J. Flis[1] and Michael G. Crilly[1]

The effect of target porosity on steady-state hydrodynamic jet penetration is examined. A simple model is developed based on compressible penetration theory and validated by comparison with hydrocode computations. The model and code results show that porosity has a significant effect on penetration depth.

INTRODUCTION

Shaped charges sometimes penetrate targets of materials that have a degree of porosity, including concrete, soils, rock and other geologic materials, propellants, and some other materials. Because of various mechanisms, the classical penetration models fail to accurately predict such penetrations. In this paper, the effect of target porosity is examined.

A hypervelocity penetration may be divided into four stages [1]:
1) The transient shock regime, which is governed by the materials' shock impedances. Since porous materials have low density and sound speed and therefore low impedance, the penetration rate during this stage is high.
2) The steady-state regime, which is governed by the equations of fluid flow. The porous volume of a target is compressed out by a strong shock, or compaction wave, that precedes the penetration zone, significantly reducing the penetration rate compared to the classical density-law's prediction.
3) Afterflow or cavitation (additional penetration after the jet is consumed), governed by target strength, which is low for porous materials. Therefore, a large contribution of afterflow is expected. Also, if the target material is significantly less dense than the jet, a substantial amount of secondary penetration may occur, especially after the jet has broken, as discussed by Held [2].
4) Recovery, which is limited by the elastic response of target. Since the elastic regime is small for porous materials, little recovery is expected.

These stages are evident in the plot of penetration vs. time predicted by a computation using the CTH code of an L/D = 15, non-porous iron jet penetrating a thick porous iron target at 4 km/s. The 38.7%-porous iron is modeled using the P-α model [3]. For about the first microsecond (transient-shock regime), the penetration velocity is about 2.4 km/s, then settles back

[1] DE Technologies, Inc., 3620 Horizon Drive, King of Prussia, PA 19406 USA

to a steady value of a little more than 2 km/s until the rod is consumed, at a time of 26 μs. After this, the hole continues to grow, or cavitate, by another 5.6 mm in depth, at a decreasing rate. No elastic recovery is observed.

Figure 2, a plot of mass-density contours at 10 μs for this computation, shows clearly the existence of the compaction wave as a steep gradient in density ahead of the penetration cavity. Behind this wave, the target material has a high density close to that of the non-porous iron jet.

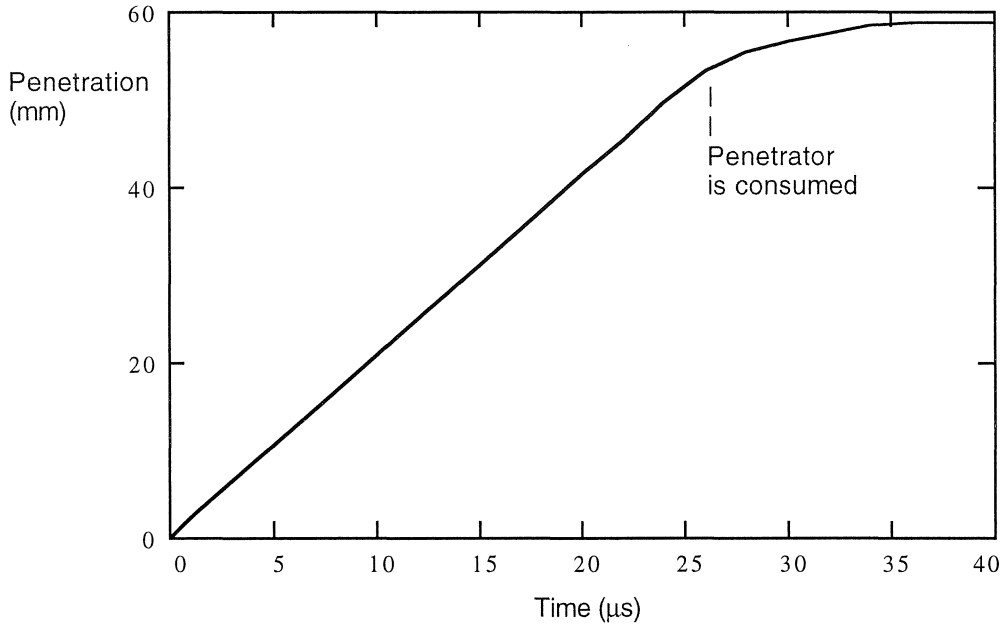

Fig. 1. Penetration depth of an iron jet into a porous-iron target vs. time.

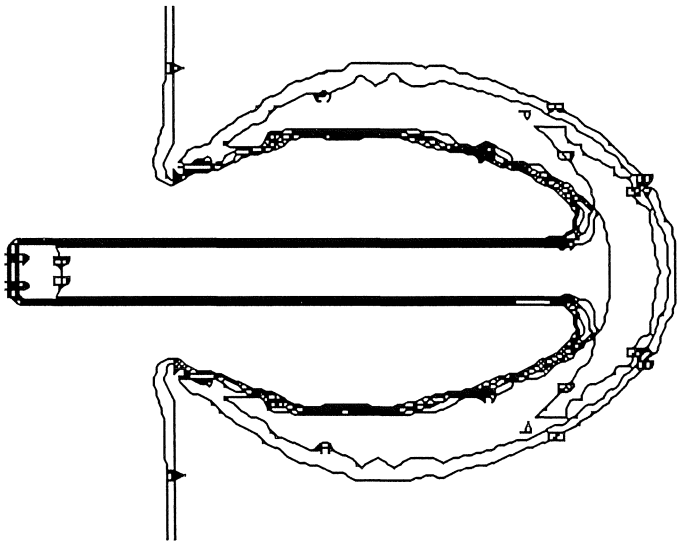

Fig. 2. Hydrocode computation of an iron jet penetrating a porous-iron target at 4 km/s shows the compaction wave ahead of the penetration zone.

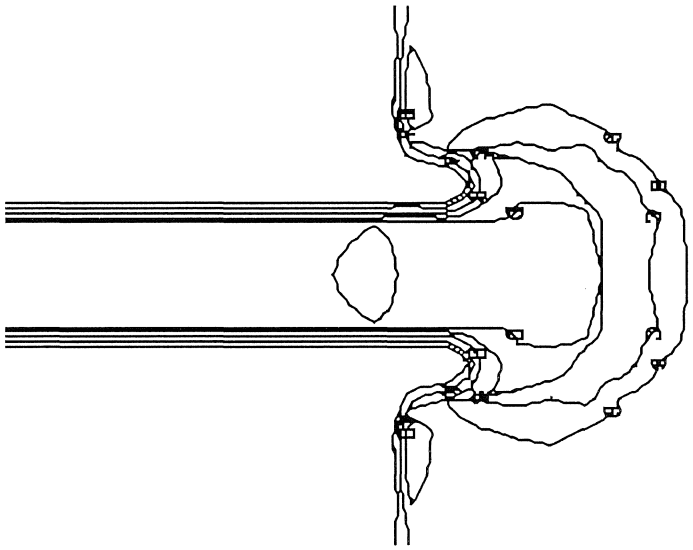

Fig. 3. Hydrocode computation of an iron jet penetrating a porous-iron target at 1 km/s shows gradual compaction ahead of the penetration zone.

For lower jet velocities (somewhat below 2 km/s for iron penetrating porous iron), however, the target is not completely compacted in a distinct wave. As shown in Fig. 3 for a jet velocity of 1 km/s, the compaction is more gradual, approaching full density only very near the jet-target interface.

This paper addresses the steady-state phase of penetration, which predominates in hypervelocity long-rod and shaped-charge-jet penetration. A model based on the compressible steady-state theory of jet penetration [4,5] is developed, with the target's porosity described by the approximate ideal-locking model and with accounting for the compaction wave in the target. The result is a surprisingly simple modification of existing penetration equations to account for porosity. The accuracy of the model is substantiated by comparison with the results of hydrocode computations.

MODEL

First, the compressible theory of jet penetration [4,5] is applied to a porous target modeled approximately as an ideal locking material, illustrated in Fig. 4. With a constant resistance R, the target is suddenly compressed to its full density in a compaction wave, which propagates ahead of the penetration zone, and beyond which it experiences no further compression (behaves incompressibly). It is assumed that the jet is incompressible, and has strength Y. (To some degree, the effects of the actual compressibilities of the jet and the fully compacted target material cancel each other.)

Stations in the jet, with velocity V, and the target, penetrated at a rate U, are defined in Fig. 5. For a quasi-steady state, the compaction wave stands in the target as a bow wave ahead of the crater. Following the notation of Flis et al. [6], the pressure in the jet at the stagnation point is given by the incompressible Bernoulli equation as

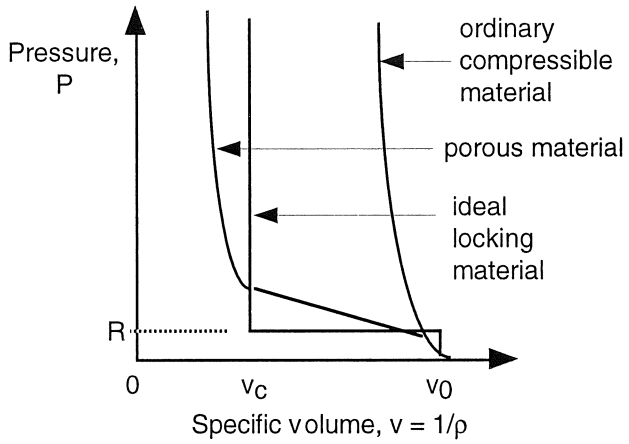

Fig. 4. Compression behavior of compressible and porous materials.

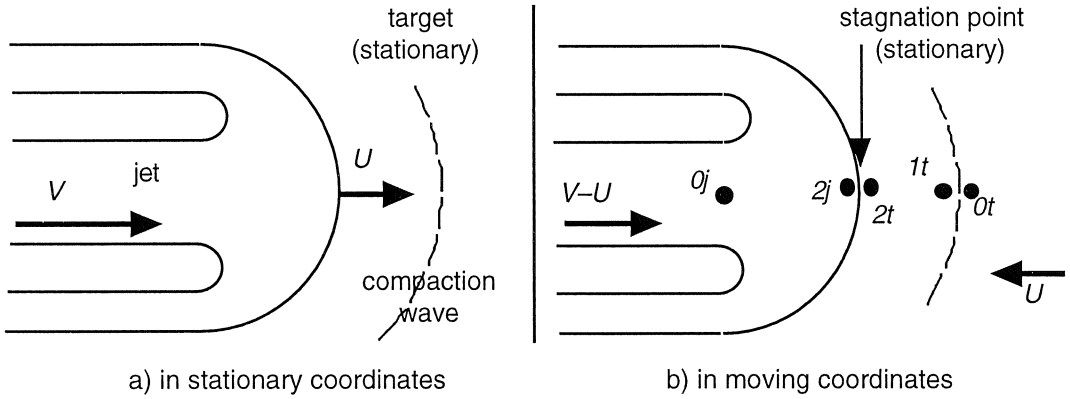

Figure 5. Steady-state jet penetration into a porous target.

$$p_{2j} = p_{0j} + \frac{1}{2}\rho_{0j}(V-U)^2 = Y + \frac{1}{2}\rho_j(V-U)^2 \tag{1}$$

In the target, the conservation conditions across the compaction wave are

Mass: $$\rho_{0t}W_{0t} = \rho_{1t}W_{1t} \tag{2}$$

Momentum: $$p_{0t} + \rho_{0t}W_{0t}^2 = p_{1t} + \rho_{1t}W_{1t}^2 \tag{3}$$

where $$\begin{aligned} p_{0t} &= R & p_{0j} &= Y \\ W_{0t} &= U & W_{0j} &= V-U \end{aligned} \tag{4}$$

are the strengths and flow velocities relative to the stagnation point in the undisturbed target and jet. If the target material is fully compressed by the compaction wave, then $\rho_{1t} = \rho_{2t} = \rho_c$, and no further compression occurs between $1t$ and $2t$, where conditions are related by the Bernoulli equation,

$$p_{2t} = p_{1t} + \frac{1}{2}\rho_{1t}W_{1t}^2 = R + \frac{1}{2}\rho_0 U^2(1+\phi) \tag{5}$$

where ϕ is the porosity, or volume fraction of pores, in the target,

$$\phi \equiv 1 - \frac{\rho_0}{\rho_c} = 1 - \frac{v_c}{v_0} \tag{6}$$

Since the jet-target interface is in equilibrium, $p_{2t} = p_{2j}$, so that

$$Y + \frac{1}{2}\rho_j (V - U)^2 = R + \frac{1}{2}\rho_0 U^2 (1 + \phi) \tag{7}$$

which may be solved for U to yield

$$U = \begin{cases} \dfrac{V}{1 - \gamma_p^2}\left(1 - \gamma_p \sqrt{1 + \dfrac{1 - \gamma_p^2}{\gamma_p^2}\dfrac{V_c^2}{V^2}}\right), & \text{for } \gamma_p \neq 1 \\ \dfrac{V}{2}\left(1 - \dfrac{V_c^2}{V^2}\right), & \text{for } \gamma_p = 1 \end{cases} \tag{8}$$

in which

$$\gamma_p \equiv \sqrt{\frac{\rho_0}{\rho_j}(1 + \phi)} = \gamma\sqrt{1 + \phi} \tag{9}$$

is a modified γ for a porous target and where

$$V_c = \sqrt{2\frac{R - Y}{\rho_j}} \tag{10}$$

is the critical jet velocity at which $U = 0$, which accounts for the strength. For high jet velocities, the strength may be neglected, especially when it is expected to be small, as in a porous material. In this case, V_c is much less than V and may be neglected, so that the penetration velocity reduces to

$$U = \frac{V}{1 + \gamma_p} \tag{11}$$

which is identical to the usual relation except for the substitution for γ by γ_p.

For a jet that does not stretch or decelerate, we have then a modified density law for the penetration P into porous materials,

$$\frac{P(porous)}{L} = \frac{U}{V - U} = \sqrt{\frac{\rho_j}{\rho_0(1 + \phi)}} = \frac{1}{\gamma_p} \tag{12}$$

This represents the *hydrodynamic limit*, the asymptote of penetration as velocity increases.

From Eq. (12), other useful formulas follow. Comparing it with the classical density law for incompressible (non-porous) penetration yields

$$\frac{P(porous\ theory)}{P(incomp.\ theory)} = \frac{\gamma}{\gamma_p} = \frac{1}{\sqrt{1 + \phi}} \tag{13}$$

which predicts that the steady-state penetration of a porous material is less than that given by the incompressible theory.

Penetration into a porous material may also be compared to that into the fully-dense matrix material (e.g., comparing porous iron to ordinary, non-porous iron),

$$\frac{P(porous\ material)}{P(fully\text{–}dense\ matl.)} = \frac{1}{\sqrt{1-\phi^2}} \tag{14}$$

This ratio reflects the effect of introducing porosity into a given material. It predicts, as expected, that penetration of a porous material is greater; however, as shown in Fig. 6, not very much greater. E.g., if 50% porosity is introduced into a material ($\phi = 0.5$), this formula predicts that penetration increases by only 15.5%, even though the target is now only half as dense.

Further, we can compare the mass efficiencies E_m of porous and fully-dense materials,

$$\frac{E_m(porous\ material)}{E_m(fully\text{–}dense\ matl.)} = \frac{\rho_c\, P(fully\text{–}dense\ matl.)}{\rho_0\, P(porous\ material)} = \sqrt{\frac{1+\phi}{1-\phi}} \tag{15}$$

This predicts that the 50%-porous material enjoys an advantage of a factor of $\sqrt{3} \sim 1.732$ in mass efficiency over the fully-dense material.

This model may also be applied to stretching jets by substituting γ_p, given by Eq. (9), for γ in any of the well-known formulas of Allison, Vitali, DiPersio, Simon, and Merendino (as summarized by Walters et al. [7]). However, since porosity affects also the target strength (and thus the hole diameter), the jet cut-off velocity (V_{min} or U_{min}) will also need to be adjusted; in addition, some accounting of the increased afterflow or secondary penetration may be necessary for broken jets, as discussed by Held [2].

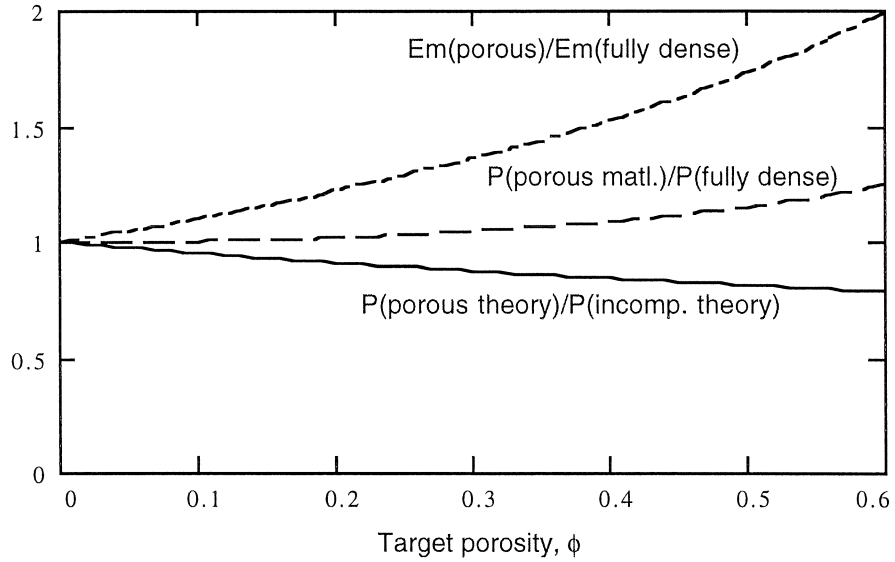

Fig. 6. Plots of the various formulas versus target porosity.

For stretching jets, the predicted effect of porosity is multiplied, relative to the density law. For example, for a jet with tip velocity twice that of its tail, penetrating a target of like material but 50% porosity, the density law

$$\frac{P}{S} = \left(\frac{V_{tip}}{V_{tail}}\right)^{1/\gamma} - 1 \tag{16}$$

where S = standoff, predicts that $P/S = 1.665$, whereas the porosity model (same equation using γ_p instead of γ) predicts a value of 1.226, 26% less. The difference is even greater for larger ratios of tip to tail velocity.

COMPARISON WITH HYDROCODE

Figure 7 compares the present model with a series of hydrocode computations similar to those described above. A porous-iron target is penetrated by an iron jet at velocities of 500 to 4000 m/s. Equation (8) with $R - Y =$ 110 MPa fits very well to the hydrocode-computed penetration rates, while the density law somewhat overpredicts. At the highest jet velocities, the porosity model predicts a penetration rate U of 0.520 times the jet velocity V, whereas the density law predicts a ratio of 0.560.

Figure 8 compares these results in terms of the ratio of penetration rate U to jet erosion rate $(V - U)$ equal to penetration per unit jet length dP/dL. This ratio emphasizes the difference between the density-law and porosity-model predictions. While the density law approaches an asymptote of 1.273, the porosity model approaches 1.083 and clearly agrees much better with the code results, not only at the highest velocities but also at 1 km/s and below, where the compaction-wave assumption is known to break down.

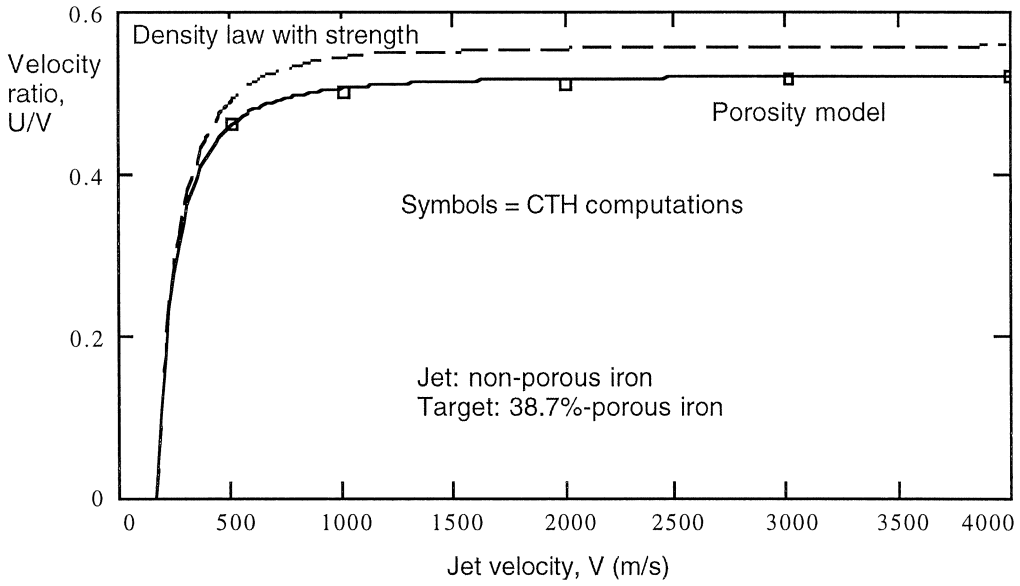

Fig. 7. Normalized penetration rate U/V for porous-iron target vs. jet velocity, computed by hydrocode, compared to density law and porosity model.

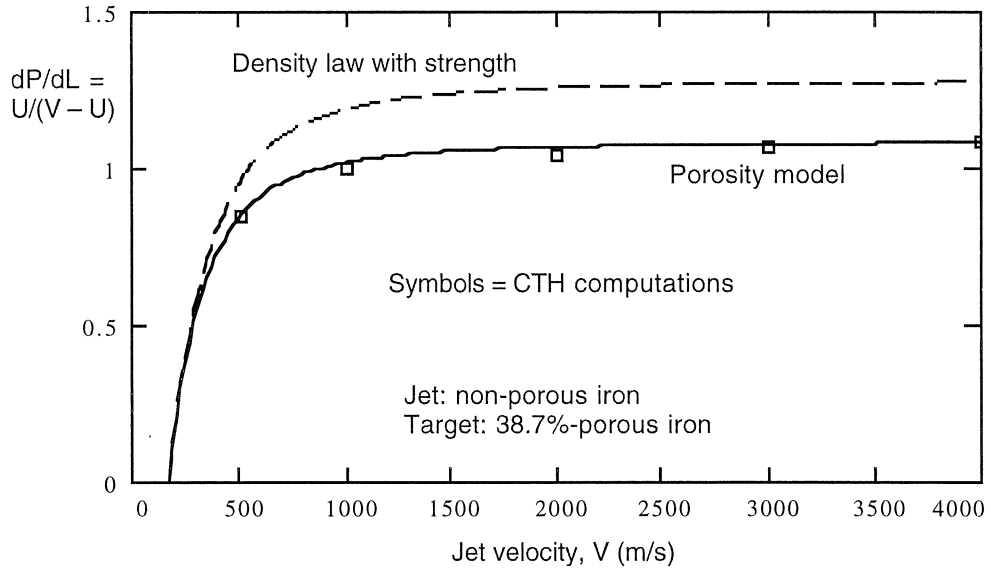

Fig. 8. Penetration per unit jet length for porous-iron target vs. jet velocity, computed by hydrocode, compared to density law and porosity model.

CONCLUSION

This paper takes a first step at addressing the effect of target porosity in hypervelocity jet penetration. Application of the quasi-steady-state compressible theory of penetration yields a simple modification of the classical density law to account for porosity. This modification is easily incorporated into all established penetration equations for stretching jets and long rod penetrators. The accuracy of this model is supported by comparison with a few hydrocode computations. Predictions of the effect of porosity based on this model are significant and quantitatively surprising.

REFERENCES

1. Gehring, J.W., C.L. Meyers, and J.A. Charest. 1965. "Experimental Studies of Impact Phenomena and Correlation with Theoretical Models," *7th Symp. Hypervel. Impact*, Tampa, FL.
2. Held, M., 1992. "Penetration of Shaped Charges in Concrete and in Sand in Comparison to Steel Targets," *J. Explosives and Propellants, R.O.C.–Taiwan*, 8(1):1-15.
3. Herrmann,W. 1970. "Constitutive Equation for the Dynamic Compaction of Ductile Porous Materials," *J. Appl. Phys.*, 40(6):2490-9.
4. Haugstad, B.S., and O.S. Dullum. 1981. "Finite compressibility in shaped charge jet and long rod penetration—the effect of shocks," *J. Appl. Phys.*, 52(8):5066-5071.
5. Flis, W.J., and P.C. Chou, "Penetration of Compressible Materials by Shaped-Charge Jets," *7th Int. Symp. Ballistics*, The Hague, The Netherlands, 19-21 April 1983.
6. Flis, W.J., M.G. Crilly, G. Hodges, and C. Vessels, 1993. "Penetration of Explosives by Shaped-Charge Jets," *14th Int. Symp. Ballistics*, Québec, Canada, 26-29 Sept. 1993.
7. Walters, W., W.J. Flis, and P.C. Chou. 1988. "A Survey of Shaped-Charge Jet Penetration Models," *Int. J. Impact Engng.*, 7(3):307-325.